Structural Changes in Bacteriorhodopsin following Retinal Photoisomerization from the 13-Cis Form†

Noriko Mizuide,‡ Mikihiro Shibata,‡ Noga Friedman,§ Mordechai Sheves,§ Marina Belenky,|| Judith Herzfeld,|| and Hideki Kandori*,‡

Department of Materials Science and Engineering, Nagoya Institute of Technology, Showa-ku, Nagoya 466-8555, Japan, Weizmann Institute of Science, Rehovot 76100, Israel, and Department of Chemistry, Brandeis University, Waltham, Massachusetts 02454-9110

Received May 15, 2006; Revised Manuscript Received July 16, 2006

ABSTRACT: Bacteriorhodopsin (BR), a light-driven proton pump in *Halobacterium salinarum*, accommodates two resting forms of the retinylidene chromophore, the all-trans form (AT-BR) and the 13-cis,15-syn form (13C-BR). Both isomers are present in thermal equilibrium in the dark, but only the all-trans form has proton-pump activity. In this study, we applied low-temperature Fourier-transform infrared (FTIR) spectroscopy to 13C-BR at 77 K and compared the local structure around the chromophore before and after photoisomerization with that in AT-BR. Strong hydrogen-out-of-plane (HOOP) vibrations were observed at 964 and 958 cm^{-1} for the K state of 13C-BR (13C-BR_K) versus a vibration at 957 cm^{-1} for the K state of AT-BR (AT-BR_K). In AT-BR_K, but not in 13C-BR_K, the HOOP modes exhibit isotope shifts upon deuteration of the retinylidene at C15 and at the Schiff base nitrogen. Whereas the HOOP modes of AT-BR_K were significantly affected by the mutation of Thr89, this was not the case for the HOOP modes of 13C-BR_K. These observations imply that, while the chromophore distortion is localized near the Schiff base in AT-BR_K, it is located elsewhere in 13C-BR_K. By use of [ζ-^{15}N]lysine-labeled BR, we identified the N−D stretching vibrations of the 13C-BR Schiff base (in D_2O) at 2173 and 2056 cm^{-1}, close in frequency to those of AT-BR. These frequencies indicate strong hydrogen bonding of the Schiff base in 13C-BR, presumably with a water molecule as in AT-BR. In contrast, the N−D stretching vibration appears at 2332 and 2276 cm^{-1} in 13C-BR_K versus values of 2495 and 2468 cm^{-1} for AT-BR_K, suggesting that the rupture of the Schiff base hydrogen bond that occurs in AT-BR_K does not occur in 13C-BR_K. Rotational motion of the Schiff base upon retinal isomerization is probably smaller in magnitude for 13C-BR than for AT-BR. These differences in the primary step are possibly related to the absence of light-driven proton pumping by 13C-BR.

Bacteriorhodopsin (BR)[1] is a light-driven proton pump in *Halobacterium salinarum* (*1*). As the most accessible ion pump, BR has been extensively studied by a wide range of methods (*2*−*13*).

The chromophore of BR is a retinylidene formed by a Schiff base linkage between the aldehyde of retinal and the amine of Lys216. Two forms of the chromophore occur in equilibrium in dark-adapted samples: all-trans (AT-BR) and 13-cis,15-syn (13C-BR) in a 1:1 to 1:2 (*14*−*16*) ratio (Figure 1). Due to the double isomerization, both forms are nearly linear and therefore accommodated by the binding pocket without undue strain. However, upon photoexcitation, AT-BR relaxes to the all-trans form, whereas 13C-BR tends to convert from the 13-cis,15-syn form to the all-trans form (*17*−*19*). Thus, a period of "light adaptation" leads to a pure AT-BR sample. Another difference is that only AT-BR has proton-pump activity. The photocycle of AT-BR comprises a series of intermediates, designated as the J, K, L, M, N, and O states, that involve translocation of a proton from the cytoplasmic side of the membrane to the extracellular side

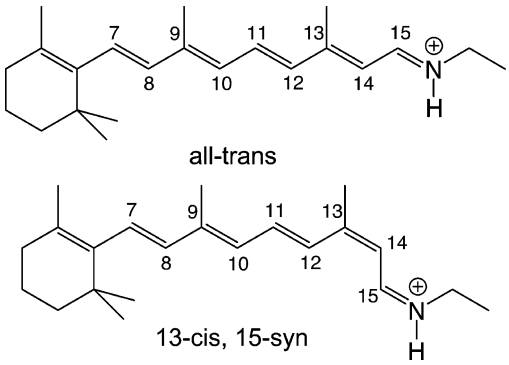

FIGURE 1: Retinylidene isomers in dark-adapted bacteriorhodopsin.

† This work was supported by grants from the Japanese Ministry of Education, Culture, Sports, Science, and Technology to H.K. and from the U.S. National Institutes of Health to J.H.

* To whom correspondence should be addressed. Phone and fax: 81-52-735-5207. E-mail: kandori@nitech.ac.jp.

‡ Nagoya Institute of Technology.

§ Weizmann Institute of Science.

|| Brandeis University.

[1] Abbreviations: BR, bacteriorhodopsin; AT-BR, bacteriorhodopsin possessing all-trans retinal as the chromophore; 13C-BR, bacteriorhodopsin possessing 13-cis,15-syn retinal as the chromophore; 13C-BR_K, K intermediate of the photocycle of 13C-BR; AT-BR_K, K intermediate of the photocycle of AT-BR; FTIR, Fourier-transform infrared; HOOP, hydrogen-out-of-plane vibration.

10.1021/bi060958s CCC: $33.50
Published on Web 08/15/2006

via Asp96, the Schiff base, Asp85, and the Glu204−Glu194 cluster. Structure−function relationships in AT-BR have been extensively studied (*2*−*13*).

In contrast, 13C-BR is not well-studied, presumably because it has no proton-pumping activity. Upon photoexcitation of 13C-BR, a red-shifted K intermediate (13C-BR_K) is formed, which is more long-lived than the K intermediate of AT-BR (AT-BR_K) (*19*, *20*). At no point in the photocycle is the Schiff base deprotonated, which is consistent with its failure to pump protons. However, X-ray crystallography indicates that the protein structure in 13C-BR is very similar to that in AT-BR (*21*, *22*). In particular, similar water-containing hydrogen-bonding networks are found at the Schiff base. These facts suggest that the chromophore configuration is the functional determinant of BR in a common protein structure and emphasize the importance of comparing structural changes in 13C-BR with those in AT-BR.

We have extensively studied structural changes in AT-BR by means of low-temperature Fourier-transform infrared (FTIR) spectroscopy (*10*, *23*). In particular, we developed measurements before and after retinal photoisomerization over the entire mid-infrared region (4000−800 cm^{-1}), including the X−H (X═O or N) and X−D (in D_2O) stretching vibrations (*24*). These vibrations are direct indicators of hydrogen-bonding strength, including that of internal water molecules and the Schiff base. By the use of isotopes ($D_2{}^{18}O$ and [ζ-^{15}N]lysine), we identified the O−D stretch of water (*25*−*28*) and the N−D stretch of the Schiff base (*29*). These results clearly show the perturbation of the hydrogen-bonding network in the Schiff base region upon photoisomerization of the all-trans chromophore to the 13-cis form.

The N−D stretching frequency is located at 2123 and 2173 cm^{-1} for AT-BR and at 2468 and 2495 for AT-BR_K (*29*). The frequency upshift of ∼300 cm^{-1} indicates significant weakening, or even complete loss, of the hydrogen bond of the Schiff base in AT-BR_K. Polarized measurement determined that the dipole moment of the N−D stretch of the Schiff base in AT-BR_K is oriented parallel to the membrane (*29*). X-ray crystallography of AT-BR_K also suggested that the N−H group is oriented parallel to the membrane (*30*, *31*). These results show the rotation of the Schiff base, and the perturbation of the hydrogen bonding in the Schiff base region, that accompanies the C13═C14 isomerization.

Analysis of water signals was more complex, because three water molecules form the center of the hydrogen-bonding network that includes several charged groups (Schiff base, Arg82, Asp85, and Asp212) and several polar groups (Tyr57, Thr89, and Tyr185) (*22*). Nevertheless, by use of various mutants, we determined that six O−D stretches in the AT-BR_K minus AT-BR spectra originate from three water molecules in the Schiff base region (*28*). It should be noted that some water bands were much lower in frequency (<2400 cm^{-1} as the O−D stretch) than those of fully hydrogen-bonded tetrahedral waters, indicating the existence of strongly hydrogen-bonded water molecules (*25*, *27*, *28*).

Upon retinal photoisomerization, hydrogen bonds of water are weakened. This is consistent with previous suggestions, based on quantum chemical and molecular mechanical calculations, that destabilization of the hydrogen bonds of water and the Schiff base plays an important role in the light-energy storage in AT-BR_K (*32*, *33*). Previous FTIR studies of BR mutants and other rhodopsins have revealed that strongly hydrogen-bonded water molecules are only found in the proteins exhibiting proton-pumping activity (*34*), suggesting an important functional role for the hydrogen bonding of water.

In this work, we examine photoinduced structural changes in 13C-BR by means of low-temperature FTIR spectroscopy. By subtracting the AT-BR_K minus AT-BR spectra from the difference spectra of dark-adapted BR, we were able to obtain the 13C-BR_K minus 13C-BR spectra. These spectra were compared with the AT-BR_K minus AT-BR spectra in various respects. Detailed analysis entailed (i) deuterating the chromophore at C15 and the Schiff base nitrogen, (ii) introducing ^{15}N at the position of lysine, (iii) exchanging with $D_2{}^{18}O$, and (iv) mutating Thr89. The results for 13C-BR_K were clearly different from those for AT-BR_K.

MATERIALS AND METHODS

Previously described methods were used to prepare [ζ-^{15}N]-lysine BR (*35*), introduce [15-^{2}H]retinal (*36*), and prepare the T89A mutant (*37*). A 120 μL aliquot of the purple membrane fraction in 2 mM phosphate buffer (pH 7.0) was dried on a BaF_2 window with a diameter of 18 mm. The completely dark-adapted sample film (in the dark at room temperature for >1 day) was then hydrated with 1 μL of H_2O, D_2O, or $D_2{}^{18}O$ under dim red light (>690 nm). The hydrated film sample was placed in a cell and then mounted in an Oxford DN-1704 cryostat on the sample holder of the FTIR spectrometer (FTS-7000).

Illumination of the dark-adapted BR with 501 nm light at 77 K for 2 min converted both AT-BR and 13C-BR into their K intermediates. Subsequent illumination of the sample with >680 nm light for 1 min reconverted AT-BR_K and 13C-BR_K into AT-BR and 13C-BR, respectively, as shown by mirror image difference spectra. The difference spectrum was calculated from spectra constructed with 256 interferograms before and after the illumination. Four spectra obtained in this way were averaged. The 13C-BR_K minus 13C-BR spectra were obtained by subtracting the AT-BR_K minus AT-BR spectra from the difference spectra for dark-adapted BR using the two marker bands of the retinal chromophore: the ethylenic C═C stretch at 1515 (+) cm^{-1} and the HOOP modes at 957 (+) cm^{-1} in H_2O [951 (+) cm^{-1} in D_2O] (see the Results for further details). The AT-BR_K minus AT-BR spectra were measured as described previously (*24*), except that polarized FTIR spectroscopy was applied in the study presented here only when specified (*38*).

RESULTS

13C-BR_K minus 13C-BR Spectra. In this study, we followed illumination of the dark-adapted BR with 501 nm light at 77 K by illumination with >680 nm light. Both AT-BR and 13C-BR are converted to their K intermediates in the first step and revert to their original states by the second step, as verified by mirror image difference spectra. Figure 2a shows the difference spectra thus obtained. Although they include both the AT-BR_K minus AT-BR and 13C-BR_K minus 13C-BR spectra, the spectra look similar to the pure AT-BR_K minus AT-BR spectra obtained from light-adapted samples (Figure 2b) in that both exhibit peaks at 1203 (−), 1194 (+), and 1167 (−) cm^{-1} in the fingerprint region. These

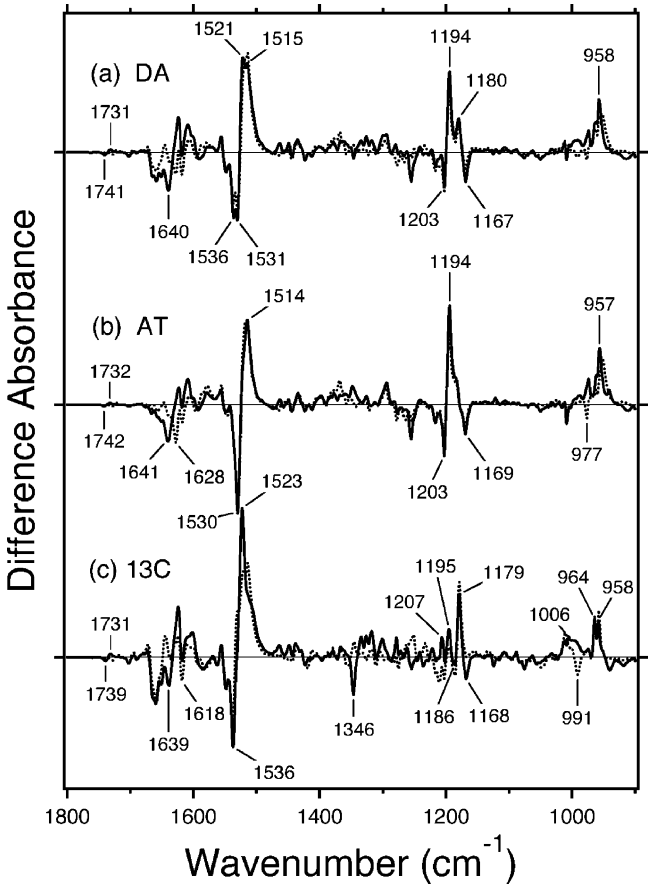

FIGURE 2: Difference FTIR spectra between the K intermediate and unphotolyzed state in the 1800−900 cm^{-1} region measured at 77 K. (a) Difference spectra for dark-adapted BR which contains AT-BR and 13C-BR, upon hydration with H_2O (—) and D_2O (···). (b) Difference spectra for light-adapted BR which contains only AT-BR, upon hydration with H_2O (—) and D_2O (···). (c) 13C-BR_K minus 13C-BR spectra obtained by subtracting the spectra in panel b from those in panel a. One division of the *y*-axis corresponds to 0.065 absorbance unit.

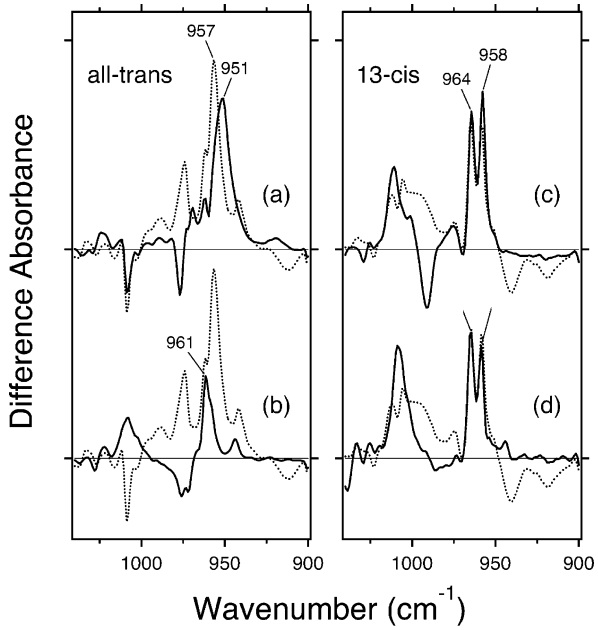

FIGURE 3: AT-BR_K minus AT-BR (a and b) and 13C-BR_K minus 13C-BR (c and d) spectra in the 1040−900 cm^{-1} region, which includes the characteristic frequencies of hydrogen-out-of-plane (HOOP) vibrations of the retinal chromophore. The unlabeled BR sample is hydrated with H_2O (dotted lines in panels a−d) and D_2O (solid lines in panels a and c), while the BR containing 15-D-labeled retinal is hydrated with H_2O (solid lines in panels b and d). One division of the *y*-axis corresponds to 0.016 absorbance unit.

are characteristic frequency changes for photoisomerization of AT-BR to AT-BR_K. However, the spectra in Figure 2a contain additional vibrational bands. For instance, Figure 2a shows the presence of a positive peak at 1180 cm^{-1}. In addition, the ethylenic C═C stretches (1550−1500 cm^{-1}) are different between panels a and b of Figure 2. Figure 2a exhibits strong bands at 1536 (−), 1531 (−), 1521 (+), and 1515 (+) cm^{-1}. Since the AT-BR_K minus AT-BR spectra (Figure 2b) possess peaks at 1530 (−)/1514 (+) cm^{-1}, the new bands at 1536 (−)/1521 (+) cm^{-1} presumably originate from the 13C-BR_K minus 13C-BR spectra.

To subtract the AT-BR_K minus AT-BR spectra (Figure 2b) from those in Figure 2a, we were initially guided by the assignments given above. As the amplitude for the AT-BR_K minus AT-BR spectrum is increased, the magnitude of the positive peak at 1515 cm^{-1} in Figure 2a is reduced, eventually yielding an unacceptable negative feature. Further discrimination is provided by a sharp HOOP band. The AT-BR_K minus AT-BR spectra possess a sharp peak at 957 cm^{-1} in H_2O (solid line), which shifts to 951 cm^{-1} in D_2O (dotted line) (more clearly seen in Figure 3a). Since the 13C-BR_K minus 13C-BR spectra also possess a positive peak in this frequency region, the spectrum in Figure 2a exhibits a peak at 958 cm^{-1} in H_2O. Subtracting the contribution of the AT-BR_K minus AT-BR spectra reduces the magnitude of the peak at 957 cm^{-1} (951 cm^{-1} in D_2O), eventually yielding an unacceptable negative feature at 955 and 948 cm^{-1} in H_2O and D_2O, respectively. By adjusting for smooth spectral features at these frequencies, we determined the 13C-BR_K minus 13C-BR spectra (Figure 2c). It is noted that although the subtraction might not be perfect, the spectral features in Figure 2c are not significantly altered, when the balance is changed. Furthermore, the spectra in Figure 2c are similar to the 13C-BR_K minus 13C-BR spectra reported previously (*39*).

In Figure 2c, the negative band at 1536 cm^{-1} corresponds to the ethylenic stretching vibration of 13C-BR, which exhibits an absorption maximum at 555 nm (*40*, *41*). The frequency is in good agreement with the well-known linear correlation between the ethylenic stretching frequencies and the frequency of the visible absorption maxima for various retinal proteins (*42*). Illumination yields a downshift to 1523 cm^{-1}, indicating formation of the red-shifted K intermediate (13C-BR_K). The positive peak seems to be downshifted in D_2O (Figure 2c), suggesting that D_2O-sensitive bands are involved in this frequency region.

C−C stretching vibrations of the retinal in the 1250−1150 cm^{-1} region are sensitive to the local structure of the chromophore. In the 13C-BR_K minus 13C-BR spectrum in H_2O, peaks are observed at 1207 (+), 1195 (+), 1186 (−), 1179 (+), and 1168 (−) cm^{-1} (Figure 2c, solid line). The appearance of a peak pair at 1186 (−) and 1179 (+) cm^{-1}, assigned to the H−D unexchangeable C10−C11 stretching vibration (*39*, *43*), was regarded as a marker of the formation of the photoproduct having the all-trans form. Therefore, 13C-BR_K presumably possesses the all-trans chromophore because of its C13═C14 photoisomerization. The 13C-BR_K minus 13C-BR spectra also possess a sharp negative peak at 1346 cm^{-1}, which disappears in D_2O (Figure 2c). This

band can be attributed to the N−H in-plane bending vibration of the Schiff base, being shifted to 991 cm^{-1} in D_2O.

Negative peaks at 1639 cm^{-1} in H_2O and 1618 cm^{-1} in D_2O probably originate from C═N stretching vibrations of the retinal Schiff base. The 21 cm^{-1} difference is larger than that for AT-BR (13 cm^{-1} in Figure 2b), suggesting that the hydrogen bond is stronger in 13C-BR than in AT-BR. This observation is consistent with NMR chemical shifts (*41*). However, it is possible for other vibrations, such as amide-I, to perturb quantitative comparison of the hydrogen-bonding strengths. In addition, the C═N stretches for 13C-BR_K on the positive side of Figure 2b are not clear. However, we have shown that the hydrogen-bonding strength of the Schiff base is more accurately described from the N−D stretch in D_2O than from the C═N stretches (*29*), and hydrogen bonding of the Schiff base will be discussed further below, with reference to the N−D stretching frequency region.

Bands in the 13C-BR_K minus 13C-BR spectra at 1739 (−)/1731 (+) cm^{-1} in H_2O (solid line in Figure 2c), which are shifted to 1727 (−)/1721 (+) cm^{-1} in D_2O (dotted line in Figure 2c), probably originate from the C═O stretching vibrations of Asp115 (*44*). The hydrogen bonding of the C═O group is slightly stronger in 13C-BR than in AT-BR, but the strengthening of the hydrogen bond upon retinal isomerization is similar.

Characteristic Hydrogen-Out-of-Plane (HOOP) Vibrations of AT-BR_K and 13C-BR_K. Hydrogen-out-of-plane (HOOP) vibrations, N−D in-plane bending, and methyl rocking vibrations are observed in the 1110−890 cm^{-1} region. Figure 3 compares the AT-BR_K minus AT-BR and 13C-BR_K minus 13C-BR spectra in the HOOP region. Strong HOOP modes represent distortion of the retinal molecule at the corresponding position (*2*, *5*, *45*−*47*). AT-BR_K possesses a strong HOOP band at 957 cm^{-1} (dotted line in Figure 3a), which was previously identified as C15-HOOP (*48*). This band is downshifted to 951 cm^{-1} in D_2O (solid line in Figure 3a), indicating that the HOOP vibration contains the Schiff base mode. The positive spectral feature in the AT-BR_K minus AT-BR spectra also changes remarkably with C15−D labeling (solid line in Figure 3b). These observations indicate that chromophore distortion in AT-BR_K originates predominantly from the Schiff base region, which is consistent with the previous study (*49*).

In the case of 13C-BR, the spectra possess two strong peaks at 964 and 958 cm^{-1} (dotted line in Figure 3c). Unlike those in AT-BR, they are not sensitive to H−D exchange (solid line in Figure 3c) or to C15−D labeling (solid line in Figure 3d). These facts indicate that the bands at 964 and 958 cm^{-1} contain neither the Schiff base mode nor the C15−H mode. They probably originate from the HOOP modes of the retinal chromophore, and although other vibrations due to protein cannot be excluded at this time, it is likely that the chromophore distortion in 13C-BR_K occurs predominantly in the polyene chain, rather than at the Schiff base region.

Distinctions in chromophore distortion between AT-BR_K and 13C-BR_K are further tested by use of a mutant protein. From X-ray crystallography, it is known that Thr89 is located near the Schiff base. In fact, the Cβ atom of Thr89 is 4.4 Å from the Schiff base nitrogen and 4.4 Å from the C15 atom of retinal in AT-BR (*22*). On the other hand, in 13C-BR, the Cβ atom of Thr89 is 4.4 Å from the Schiff base nitrogen and 5.1 Å from the C15 atom of retinal (*21*). Therefore, if the structural changes of the retinal chromophore occur near the Schiff base in AT-BR, but not in 13C-BR, we expect that mutation at Thr89 will affect the HOOP modes of AT-BR_K more significantly than those of 13C-BR_K. This was indeed the case. Figure 4 compares the HOOP vibrations between the wild type (dotted lines) and T89A mutant (solid lines) in H_2O. The HOOP mode of the AT-BR_K minus AT-BR spectra that occurs at 957 cm^{-1} in the wild type appears to be shifted to 945 cm^{-1} in T89A (Figure 4a). In contrast, mutation produced almost no spectral changes for the bands at 964 and 958 cm^{-1} in the 13C-BR_K minus 13C-BR spectra (Figure 4b). Thus, the distortions of the retinal chromophore probably occur near the Schiff base in AT-BR, but not in 13C-BR.

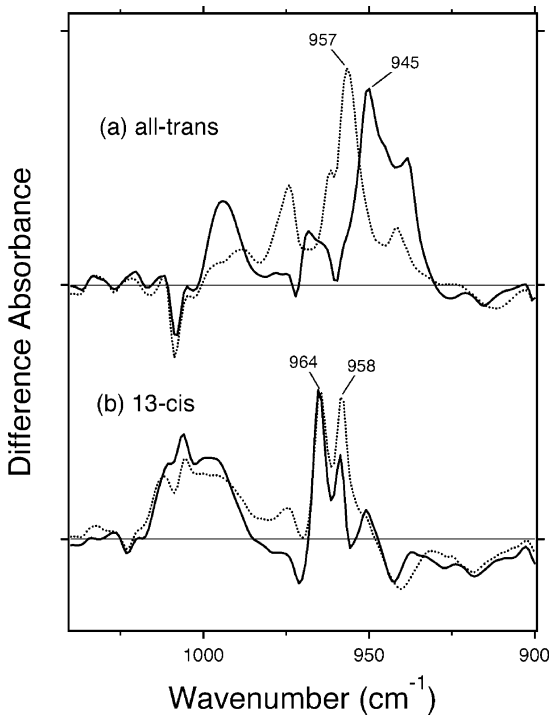

FIGURE 4: AT-BR_K minus AT-BR (a) and 13C-BR_K minus 13C-BR (b) spectra in the 1040−900 cm^{-1} region. The wild-type (···) and T89A (−) samples are hydrated with H_2O. One division of the *y*-axis corresponds to 0.017 absorbance unit.

Assignment of the N−D Stretching Vibrations of the Schiff Base in 13C-BR and AT-BR. X−D stretching vibrations of protein and water molecules appear in the 2750−2000 cm^{-1} region for films hydrated with D_2O. The solid line in Figure 5a shows the AT-BR_K minus AT-BR spectrum, which reproduced the previous results (*29*). On the other hand, the 13C-BR_K minus 13C-BR spectrum (the solid line in Figure 5b) is obtained for the first time. Since the N−D stretching vibration of the Schiff base is in this frequency region, we used the [ζ-^{15}N]lysine-labeled BR sample for assignment.

Figure 5a compares the AT-BR_K minus AT-BR spectra for [ζ-^{15}N]lysine-labeled (dotted line) and unlabeled (solid line) BR. As reported previously (*29*), an isotope-induced downshift was observed for the two negative bands at 2173 and 2123 cm^{-1}, indicating that the bands originate from N−D stretching vibrations of the Schiff base in AT-BR. [ζ-^{15}N]-Lysine-induced shifts were also observed for the two positive spectral features at 2495 and 2468 cm^{-1}, corresponding to

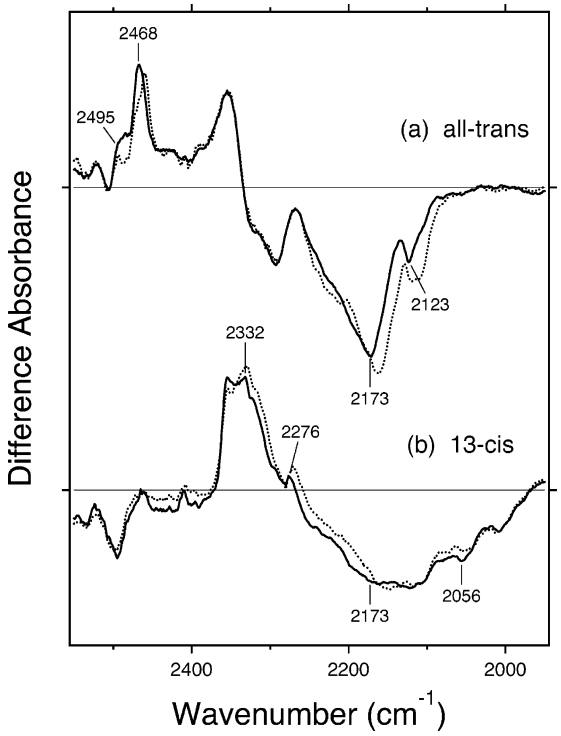

FIGURE 5: AT-BR_K minus AT-BR (a) and 13C-BR_K minus 13C-BR (b) spectra in the 2550−1950 cm^{-1} region. Solid and dotted lines represent the spectra for the unlabeled and [ζ-^{15}N]lys-labeled BR, respectively, in D_2O. One division of the *y*-axis corresponds to 0.003 absorbance unit. Labeled frequencies correspond to the N−D stretching vibrations of the protonated Schiff base.

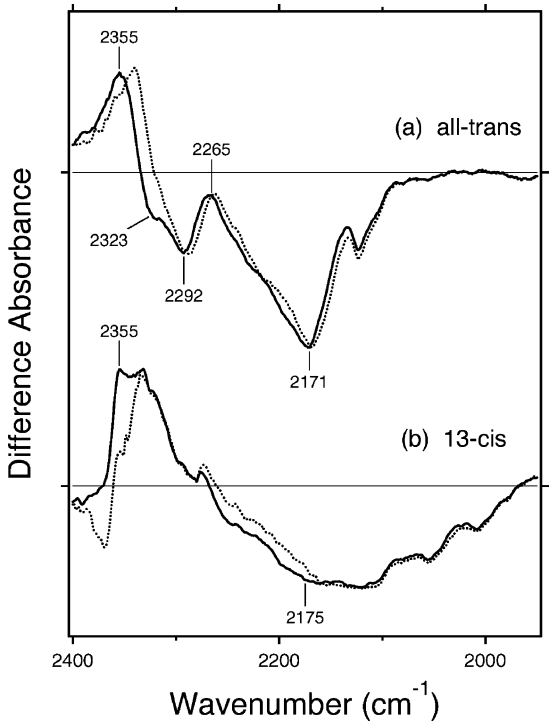

FIGURE 6: AT-BR_K minus AT-BR (a) and 13C-BR_K minus 13C-BR (b) spectra in the 2400−1950 cm^{-1} region. The sample was hydrated with D_2O (—) or $D_2{}^{18}O$ (•••). One division of the *y*-axis corresponds to 0.003 absorbance unit. Labeled frequencies correspond to O−D stretching vibrations of water molecules.

the N−D stretching vibrations of the Schiff base in AT-BR_K. In this region, the O−D frequency of Thr89 in AT-BR_K is located at 2466 cm^{-1} (as a positive band) (*50*). Since the O−D stretch is highly dichroic, the band is not clearly visible under the experimental conditions described here (with no dichroic measurements).

Figure 5b compares the 13C-BR_K minus 13C-BR spectra for [ζ-^{15}N]lysine-labeled (dotted line) and unlabeled (solid line) BR. A clear isotope-induced downshift was observed for the positive bands at 2332 and 2276 cm^{-1} and the negative bands at 2173 and 2056 cm^{-1}. Other bands are identical between [ζ-^{15}N]lysine-labeled and unlabeled 13C-BR. Thus, we are able to conclude that the N−D stretching vibrations of the Schiff base are involved in this frequency region.

By use of [ζ-^{15}N]lysine-labeled BR, we identified the N−D stretching vibrations of the Schiff base at 2173 and 2123 cm^{-1} for AT-BR and at 2173 and 2056 cm^{-1} for 13C-BR. This indicates that the hydrogen-bonding strength is only slightly greater in 13C-BR than in AT-BR. A similar hydrogen bond between AT-BR and 13C-BR is consistent with the water near the Schiff base in both X-ray structures (*21*, *22*).

We also identified the N−D stretching vibrations of the Schiff base at 2495 and 2468 cm^{-1} for AT-BR_K and at 2332 and 2276 cm^{-1} for 13C-BR_K. Upshifted N−D frequencies indicate that retinal isomerization weakens the hydrogen bond of the Schiff base in both AT-BR and 13C-BR. However, the large difference in frequencies for the K states implies a difference in the isomerization in AT-BR and 13C-BR. In case of AT-BR, the upshift upon photoisomerization is >300 cm^{-1}, indicating that the hydrogen bond is significantly weakened (or broken) in AT-BR_K presumably because of rotation of the Schiff base. In contrast, the upshift upon photoisomerization is <200 cm^{-1} for 13C-BR. This suggests that the rotation of the Schiff base that accompanies retinal isomerization is smaller in 13C-BR than in AT-BR. This observation is fully consistent with the inference from that HOOP mode that the polyene chain is distorted for 13C-BR_K.

O−D Stretching Vibrations of Water in 13C-BR and AT-BR. A spectral comparison between the samples hydrated with D_2O and $D_2{}^{18}O$ identifies O−D stretching vibrations of water molecules that change their frequencies upon retinal photoisomerization. We previously reported the results of the water O−D stretch for AT-BR (*25*−*28*). How does 13C-BR compare? Figure 6 shows difference FTIR spectra in the 2400−1950 cm^{-1} region, where strongly hydrogen-bonded water molecules are observed. The negative 2171 cm^{-1} band for AT-BR in Figure 6a was previously assigned to the O−D stretch of the bridging water molecule between the Schiff base and Asp85 (*28*). In Figure 6b, an O−D stretching vibration of water was observed at a similar frequency (2175 cm^{-1}) for 13C-BR. This suggests that the water band in 13C-BR originates from the bridging water molecule between the Schiff base and Asp85 as well as AT-BR. The pentagonal cluster structure is probably formed in the Schiff base region through similar hydrogen bonds between 13C-BR and AT-BR. The presence of the positive water band at 2355 cm^{-1} indicates that the hydrogen bond of the water is weakened upon photoisomerization in 13C-BR, as in AT-BR. In spite of these similarities, there are fewer strongly hydrogen-bonded water molecules in 13C-BR than in AT-BR. This

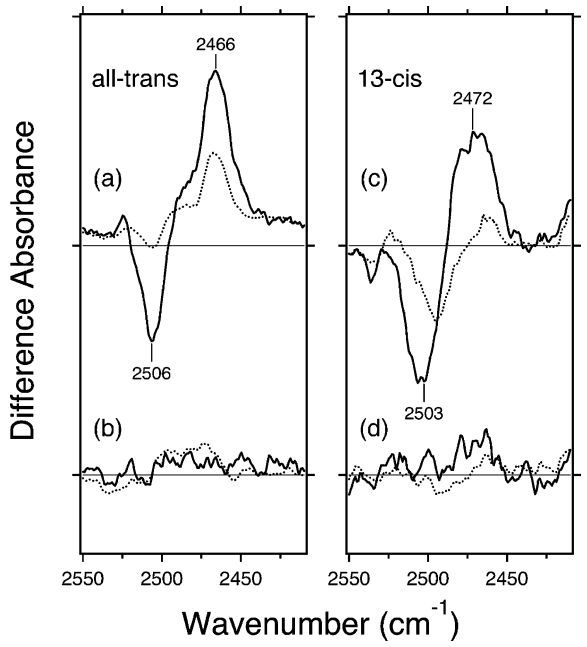

FIGURE 7: Polarized FTIR difference spectra in the 2550−2410 cm^{-1} region: (a and b) AT-BR_K minus AT-BR and (c and d) 13C-BR_K minus 13C-BR. The window tilting angles are 0° (•••) and 53.5° (—). The wild-type (a and c) and T89A mutant protein (b and d) are hydrated with D_2O. One division of the *y*-axis corresponds to 0.002 absorbance unit.

may be interpreted in terms of a small perturbation of the hydrogen-bonding network in 13C-BR, which is seen for the less altered N−D stretching vibration in 13C-BR_K (Figure 5).

O−D Stretching Vibrations of Thr89 in 13C-BR and AT-BR. The O−H stretching vibration of Thr89 is H/D exchangeable, and the highly dichroic O−D stretch in D_2O is located at 2506 cm^{-1} in AT-BR (*50*−*52*). Figure 7a shows the polarized AT-BR_K minus AT-BR FTIR spectra of the wild type, where the sample window was tilted by 0° (dotted line) and 53.5° (solid line). The bands at 2506 (−)/2466 (+) cm^{-1} increase in intensity when the window is tilted, indicating that the dipole moment is parallel to the membrane normal. The disappearance of the bands in the T89A mutant protein (Figure 7b) is consistent with the assignment to the O−D stretching vibrations of Thr89 (*50*). Similar results were obtained for 13C-BR. The polarized 13C-BR_K minus 13C-BR FTIR spectra of the wild type (Figure 7c) show the presence of highly dichroic bands at 2503 (−)/2472 (+) cm^{-1}. Since the bands completely disappeared in the T89A mutant protein (Figure 7d), the bands also originate from the O−D stretching vibrations of Thr89. Frequencies and dichroic properties are similar for the O−D stretch of Thr89 between AT-BR and 13C-BR. These results suggest that the hydrogen bond of Thr89 and its changes are similar in AT-BR and 13C-BR.

DISCUSSION

In this study, we compared the 13C-BR_K minus 13C-BR and AT-BR_K minus AT-BR spectra by means of low-temperature FTIR spectroscopy. Although the dark-adapted BR contains both 13C-BR and AT-BR, appropriate subtraction derived the 13C-BR_K minus 13C-BR spectra. The spectral comparisons were interpreted in terms of structural changes induced by photoisomerization. In addition, vibrational bands were identified by deuteration of C15 in the chromophore, ^{15}N labeling of Cζ in the lysines, hydration with $D_2{}^{18}O$, and site-directed mutagenesis of Thr89.

Unphotolyzed State of 13C-BR. We identified the N−D stretching vibration of the Schiff base at 2173 and 2056 cm^{-1} for 13C-BR (Figure 5b). We previously identified the N−D stretching vibration of the Schiff base at 2173 and 2123 cm^{-1} for AT-BR (*29*). The similarity indicates that the hydrogen-bonding strength is essentially similar, though slightly stronger in 13C-BR than in AT-BR. X-ray crystallographic structures of 13C-BR (*21*) and AT-BR (*22*) both reported the presence of a water molecule in contact with the Schiff base. Therefore, these spectroscopic results suggest that the water molecule is at least as good as a hydrogen bond acceptor for the protonated Schiff base in 13C-BR as in AT-BR.

According to the X-ray structure, the $N-O_{water}-O_{Asp85}$ (the Schiff base nitrogen, water oxygen, and carboxyl oxygen of Asp85, respectively) angles are 100° and 106° in 13C-BR and AT-BR, respectively. Therefore, if the water oxygen fully accepts the hydrogen bond of the Schiff base, the O−H group of water points toward the oxygen of Asp85 in both forms of BR. This is consistent with our inference of a strongly hydrogen-bonded water in both 13C-BR and AT-BR, from the water O−D stretch at 2175 and 2171 cm^{-1}, respectively. The similarity strongly suggests that these bands come from the bridged water stretch pointing toward Asp85.

Previous FTIR studies of BR mutants and other rhodopsins have revealed that strongly hydrogen-bonded water molecules are only found in the proteins exhibiting proton-pumping activity (*34*). This suggests that a strongly hydrogen-bonded water molecule that bridges the Schiff base and its counterion is essential for the proton-pumping function. This study also showed the presence of such a water molecule for 13C-BR, although 13C-BR does not pump protons. This exception suggests the importance of the retinal configuration, and the mechanism of photoisomerization is presumably important as well. It should be noted, however, that there are reports that 13C-BR produces an M state (*53*) and pumps protons (*54*) at alkaline pH. Although our FTIR study was conducted at neutral pH, the effect of higher pH on the Schiff base deprotonation must be at a stage later than the K state in the photocycle. The presence of a strongly hydrogen-bonded water molecule in 13C-BR may explain the partial ability of the proton-pump function, though it is much weaker than AT-BR.

Photoisomerization of 13C-BR in Comparison with That of AT-BR. After the absorption of light, photoisomerization in 13C-BR probably takes place at the C13═C14 bond, leading from the 13-cis,15-syn form to the all-trans,15-syn form. It is generally accepted that the primary K intermediate is in a high-energy state for retinal proteins. Chromophore distortion is one of the characteristic features of such a high-energy state, and HOOP vibrations monitor the chromophore distortion. Analysis of HOOP modes for 13C-BR_K and AT-BR_K (Figures 3 and 4) indicates that the chromophore distortion is less localized in the Schiff base and C15 region in 13C-BR_K than in AT-BR_K.

The N−D stretching frequency of the Schiff base in 13C-BR_K (2332 and 2276 cm^{-1}) is much lower than in AT-BR_K (2495 and 2468 cm^{-1}), though they are similar in the

unphotolyzed states. We thus inferred that the hydrogen bond of the Schiff base is cleaved in AT-BR_K, but not in 13C-BR_K. Whereas the hydrogen-bonding network is destabilized in AT-BR_K, the structural perturbation of the Schiff base region is smaller in magnitude in 13C-BR_K, where the effects of isomerization are distributed more widely.

Previous studies have attributed the lack of light-induced Schiff base deprotonation in 13C-BR to an insufficient change in the relative pK_a of the donor (Schiff base) and acceptor (Asp85) groups and/or to a high activation barrier for the proton transfer (*55*). It was shown that the required change in the relative pK_a may be achieved either by deprotonation of a protein moiety with a pK_a of ~8.5 or by intrinsically lowering the retinal Schiff base pK_a by fluorine substitution. In addition, both the protein residue titration and the fluorine substitution may reduce the barrier for proton transfer. This study, indicating that structural perturbation in the Schiff base region is smaller in magnitude in 13C-BR_K than in AT-BR_K, is in keeping with the proposal of insufficient change in the relative pK_a of the donor and acceptor groups in the photocycle of 13C-BR.

ACKNOWLEDGMENT

We thank Dr. Y. Furutani and T. Tanimoto for their help in experiments.

REFERENCES

1. Oesterhelt, D., and Stoeckenius, W. (1971) Rhodopsin-like protein from the purple membrane of *Halobacterium halobium*, *Nat. New Biol. 233*, 149−152.
2. Mathies, R. A., Lin, S. W., Ames, J. B., and Pollard, W. T. (1991) From femtoseconds to biology: Mechanism of bacteriorhodopsin's light-driven proton pump, *Annu. Rev. Biophys. Biophys. Chem. 20*, 491−518.
3. Krebs, M. P., and Khorana, H. G. (1993) Mechanism of light-dependent proton translocation by bacteriorhodopsin, *J. Bacteriol. 175*, 1555−1560.
4. Lanyi, J. K., and Váró, G. (1995) The photocycles of bacteriorhodopsin, *Isr. J. Chem. 35*, 365−385.
5. Maeda, A. (1995) Application of FTIR spectroscopy to the structural study on the function of bacteriorhodopsin, *Isr. J. Chem. 35*, 387−400.
6. Moltke, S., Alexiev, U., and Heyn, M. P. (1995) Kinetics of light-induced intramolecular charge transfer and proton release in bacteriorhodopsin, *Isr. J. Chem. 35*, 401−414.
7. Balashov, S. P. (1995) Photoreactions of the photointermediates of bacteriorhodopsin, *Isr. J. Chem. 35*, 415−428.
8. Honig, B., Ottolenghi, M., and Sheves, M. (1995) Acid-base equilibria and the proton pump in bacteriorhodopsin, *Isr. J. Chem. 35*, 429−446.
9. Haupts, U., Tittor, J., and Oesterhelt, D. (1999) Closing in on bacteriorhodopsin: Progress in understanding the molecules, *Annu. Rev. Biophys. Biomol. Struct. 28*, 367−399.
10. Kandori, H. (2000) Role of internal water molecules in bacteriorhodopsin, *Biochim. Biophys. Acta 1460*, 177−191.
11. Herzfeld, J., and Lansing, J. C. (2002) Magnetic resonance studies of the bacteriorhodopsin pump cycle, *Annu. Rev. Biophys. Biomol. Struct. 31*, 73−95.
12. Luecke, H., and Lanyi, J. K. (2003) Structural clues to the mechanism of ion pumping in bacteriorhodopsin, *Adv. Protein Chem. 63*, 111−130.
13. Lanyi, J. K. (2004) Bacteriorhodopsin, *Annu. Rev. Physiol. 66*, 665−688.
14. Maeda, A., Iwasa, T., and Yoshizawa, T. (1977) Isomeric composition of retinal chromophore in dark-adapted bacteriorhodopsin, *J. Biochem. 82*, 1599−1604.
15. Stoeckenius, W., Lozier, R. H., and Bogomolni, R. A. (1979) Bacteriorhodopsin and the purple membrane of halobacteria, *Biochim. Biophys. Acta 505*, 215−278.
16. Scherrer, P., Mathew, M. K., Sperling, W., and Stoeckenius, W. (1989) Retinal isomer ratio in dark-adapted purple membrane and bacteriorhodopsin monomers, *Biochemistry 28*, 829−834.
17. Tokunaga, F., Iwasa, T., and Yoshizawa, T. (1976) Photochemical reaction of bacteriorhodopsin, *FEBS Lett. 72*, 33−38.
18. Sperling, W., Carl, P., Rafferty, C. N., and Dencher, N. A. (1977) Photochemistry and dark equilibrium of retinal isomers and bacteriorhodopsin isomers, *Biophys. Struct. Mech. 3*, 79−94.
19. Kalisky, O., Goldschmidt, C. R., and Ottolenghi, M. (1977) On the photocycle and light adaptation of dark-adapted bacteriorhodopsin, *Biophys. J. 19*, 185−189.
20. Hofrichter, J., Henry, E. R., and Lozier, R. H. (1989) Photocycles of bacteriorhodopsin in light- and dark-adapted purple membrane studied by time-resolved absorption spectroscopy, *Biophys. J. 56*, 693−706.
21. Nishikawa, T., Murakami, M., and Kouyama, T. (2005) Crystal structure of the 13-cis isomer of bacteriorhodopsin in the dark-adapted state, *J. Mol. Biol. 352*, 319−328.
22. Luecke, H., Schobert, B., Richter, H.-T., Cartailler, J. P., and Lanyi, J. K. (1999) Structure of bacteriorhodopsin at 1.55 Å resolution, *J. Mol. Biol. 291*, 899−911.
23. Kandori, H. (2004) Hydration switch model for the proton transfer in the Schiff base region of bacteriorhodopsin, *Biochim. Biophys. Acta 1658*, 72−79.
24. Kandori, H., Kinoshita, N., Shichida, Y., and Maeda, A. (1998) Protein structural changes in bacteriorhodopsin upon photoisomerization as revealed by polarized FTIR spectroscopy, *J. Phys. Chem. B 102*, 7899−7905.
25. Kandori, H., and Shichida, Y. (2000) Direct observation of the bridged water stretching vibrations inside a protein, *J. Am. Chem. Soc. 122*, 11745−11746.
26. Tanimoto, T., Furutani, Y., and Kandori, H. (2003) Structural changes of water in the Schiff base region of bacteriorhodopsin: Proposal of a hydration switch model, *Biochemistry 42*, 2300−2306.
27. Shibata, M., Tanimoto, T., and Kandori, H. (2003) Water molecules in the Schiff base region of bacteriorhodopsin, *J. Am. Chem. Soc. 125*, 13312−13313.
28. Shibata, M., and Kandori, H. (2005) FTIR studies of internal water molecules in the Schiff base region of bacteriorhodopsin, *Biochemistry 44*, 7406−7413.
29. Kandori, H., Belenky, M., and Herzfeld, J. (2002) Vibrational frequency and dipolar orientation of the protonated Schiff base in bacteriorhodopsin before and after photoisomerization, *Biochemistry 41*, 6026−6031.
30. Schobert, B., Cupp-Vickery, J., Hornak, V., Smith, S. O., and Lanyi, J. K. (2002) Crystallographic Structure of the K Intermediate of Bacteriorhodopsin: Conservation of Free Energy after Photoisomerization of the Retinal, *J. Mol. Biol. 321*, 715−726.
31. Matsui, Y., Sakai, K., Murakami, M., Shiro, Y., Adachi, S., Okumura, H., and Kouyama, T. (2002) Specific Damage Induced by X-ray Radiation and Structural Changes in the Primary Photoreaction of Bacteriorhodopsin, *J. Mol. Biol. 324*, 469−481.
32. Hayashi, S., Tajkhorshid, E., and Schulten, K. (2002) Structural changes during the formation of early intermediates in the bacteriorhodopsin photocycle, *Biophys. J. 83*, 1281−1297.
33. Hayashi, S., Tajkhorshid, E., Kandori, H., and Schulten, K. (2004) Role of hydrogen-bond network in energy storage of bacteriorhodopsin's light-driven proton pump revealed by ab initio normal-mode analysis, *J. Am. Chem. Soc. 126*, 10516−10517.
34. Furutani, Y., Shibata, M., and Kandori, H. (2005) Strongly hydrogen-bonded water molecules in the Schiff base region of rhodopsins, *Photochem. Photobiol. Sci. 4*, 661−666.
35. Hu, J. G., Sun, B. Q., Bizounok, M., Hatcher, M. E., Lansing, J. C., Raap, J., Verdegem, P. J. E., Lugtenburg, J., Griffin, R. G., and Herzfeld, J. (1998) Early and late M intermediates in the bacteriorhodopsin photocycle: A solid-state NMR study, *Biochemistry 37*, 8088−8096.
36. Ottolenghi, M., and Sheves, M. (1989) Synthetic retinals as probes for the binding site and photoreactions in rhodopsins, *J. Membr. Biol. 112*, 193−212.
37. Needleman, R., Chang, M., Ni, B., Váró, G., Fornés, J., White, S. H., and Lanyi, J. K. (1991) Properties of Asp^{212}→Asn bacteriorhodopsin suggest that Asp^{212} and Asp^{85} both participate in a counterion and proton acceptor complex near the Schiff base, *J. Biol. Chem. 266*, 11478−11484.
38. Tanimoto, T., Shibata, M., Belenky, M., Herzfeld, J., and Kandori, H. (2004) Altered hydrogen bonding of Arg82 during the proton

pump cycle of bacteriorhodopsin: A low-temperature polarized FTIR spectroscopic study, *Biochemistry 43*, 9439−9447.
39. Roepe, P. D., Ahl, P. L., Herzfeld, J., Lugtenburg, J., and Rothschild, K. J. (1988) Tyrosine protonation changes in bacteriorhodopsin. A Fourier transform infrared study of BR548 and its primary photoproduct, *J. Biol. Chem. 263*, 5110−5117.
40. Smith, S. O., Myers, A. B., Pardoen, J. A., Winkel, C., Mulder, P. P. J., Lugtenburg, J., and Mathies, R. A. (1984) Determination of retinal Schiff base configuration in bacteriorhodopsin, *Proc. Natl. Acad. Sci. U.S.A. 81*, 2055−2059.
41. Harbison, G. S., Smith, S. O., Pardoen, J. A., Mulder, P. P. J., Lugtenburg, J., Herzfeld, J., Mathies, R. A., and Griffin, R. G. (1984) Dark-adapted bacteriorhodopsin contains 13-cis, 15-syn and all-trans, 15-anti retinal Schiff bases, *Proc. Natl. Acad. Sci. U.S.A. 81*, 1706−1709.
42. Aton, B., Doukas, A. G., Callender, R. H., Becher, B., and Ebrey, T. G. (1977) Resonance Raman studies of the purple membrane, *Biochemistry 16*, 2995−2999.
43. Smith, S. O., Pardoen, J. A., Lugtenburg, J., and Mathies, R. A. (1987) Vibrational analysis of the 13-cis-retinal chromophore in dark-adapted bacteriorhodopsin, *J. Phys. Chem. 91*, 804−819.
44. Braiman, M. S., Mogi, T., Marti, T., Stern, L. J., Khorana, H. G., and Rothschild, K. J. (1988) Vibrational spectroscopy of bacteriorhodopsin mutants: Light-driven proton transport involves protonation changes of aspartic acid residues 85, 96, and 212, *Biochemistry 27*, 8516−8520.
45. Rothschild, K. J. (1992) FTIR difference spectroscopy of bacteriorhodopsin: Toward a molecular model, *J. Bioenerg. Biomembr. 24*, 147−167.
46. Siebert, F. (1995) Infrared spectroscopy applied to biochemical and biological problems, *Methods Enzymol. 246*, 501−526.
47. Gerwert, K. (1999) Molecular reaction mechanisms of proteins monitored by time-resolved FTIR-spectroscopy, *Biol. Chem. 380*, 931−935.
48. Maeda, A., Sasaki, J., Pfefferle, J. M., Shichida, Y., and Yoshizawa, T. (1991) Fourier transform infrared spectral studies on the Schiff base mode of all-trans bacteriorhodopsin and its photointermediates, K and L, *Photochem. Photobiol. 54*, 911−921.
49. Gat, Y., Grossjean, M., Pinevsky, I., Takei, H., Rothman, Z., Sigrist, H., Lewis, A., and Sheves, M. (1992) Participation of bacteriorhodopsin active-site lysine backbone in vibrations associated with retinal photochemistry, *Proc. Natl. Acad. Sci. U.S.A. 89*, 2434−2438.
50. Kandori, H., Kinoshita, N., Yamazaki, Y., Maeda, A., Shichida, Y., Needleman, R., Lanyi, J. K., Bizounok, M., Herzfeld, J., Raap, J., and Lugtenburg, J. (1999) Structural change of threonine 89 upon photoisomerization in bacteriorhodopsin as revealed by polarized FTIR spectroscopy, *Biochemistry 38*, 9676−9683.
51. Kandori, H., Kinoshita, N., Yamazaki, Y., Maeda, A., Shichida, Y., Needleman, R., Lanyi, J. K., Bizounok, M., Herzfeld, J., Raap, J., and Lugtenburg, J. (2000) Local and Distant Protein Structural Changes on Photoisomerization of the Retinal in Bacteriorhodopsin, *Proc. Natl. Acad. Sci. U.S.A. 97*, 4643−4648.
52. Kandori, H., Yamazaki, Y., Shichida, Y., Raap, J., Lugtenburg, J., Belenky, M., and Herzfeld, J. (2001) Tight Asp-85-Thr-89 association during the pump switch of bacteriorhodopsin, *Proc. Natl. Acad. Sci. U.S.A. 98*, 1571−1576.
53. Drachev, L. A., Dracheva, S. V., and Kaulen, A. D. (1993) pH dependence of the formation of an M-type intermediate in the photocycle of 13-cis-bacteriorhodopsin, *FEBS Lett. 332*, 67−70.
54. Kaulen, A. D., Drachev, L. A., and Zorina, V. V. (1990) Proton transport and M-type intermediate formation by 13-cis-bacteriorhodopsin, *Biochim. Biophys. Acta 1018*, 103−113.
55. Steinberg, G., Sheves, M., Bressler, S., and Ottolenghi, M. (1994) Factors affecting the formation of an M-like intermediate in the photocycle of 13-cis-bacteriorhodopsin, *Biochemistry 33*, 12439−12450.

BI060958S